ChemComm

This article is part of the

Surface Enhanced Raman Spectroscopy web themed issue

Guest editors: Professors Duncan Graham, Zhongqun Tian and Richard Van Duyne

All articles in this issue will be gathered together online at www.rsc.org/sers.

ChemComm

Dynamic Article Links

Cite this: *Chem. Commun.*, 2011, **47**, 3553–3555

www.rsc.org/chemcomm

COMMUNICATION

Functionalized Ag nanoparticles with tunable optical properties for selective protein analysis†‡

Arumugam Sivanesan, H. Khoa Ly, Jacek Kozuch, Murat Sezer, Uwe Kuhlmann, Anna Fischer and Inez M. Weidinger*

Received 19th November 2010, Accepted 31st January 2011
DOI: 10.1039/c0cc05058j

We present a preparation procedure for small sized biocompatibly coated Ag nanoparticles with tunable surface plasmon resonances. The conditions were optimised with respect to the resonance Raman signal enhancement of heme proteins and to the preservation of the native protein structure.

Surface plasmon resonances (SPR) of noble metal nanoparticles are able to enhance the oscillating electric field of incident light. This near-field enhancement can be used to selectively detect and analyse molecules in the vicinity of the metal surface. SER (*surface enhanced Raman*) spectroscopy is the most prominent analytical technique exploiting this effect since it can provide structural information about the adsorbates. The sensitivity of this approach can be further increased for molecules with electronic transitions in the visible spectral range. In this case, optimum enhancement of the Raman signals can be achieved if the excitation line is in resonance with both the SPR and the electronic transition of the immobilised molecules (SERR—*surface enhanced resonance Raman*). Thus, the central challenge is to tune the optical properties of metal nanoparticles such that the SPR coincides with the electronic transition of the adsorbate. The SPR position of noble metal nanoparticles such as Ag and Au can be controlled by variation of particle size, shape and dielectric encapsulation.[1,2] However, the spectral tuning of Au is restricted to wavelengths larger than 500 nm[1] such that this metal is not applicable for SERR spectroscopy of chromophores in the blue and violet regions. Ag nanoparticles (AgNPs) exhibit plasmon resonances up to the near UV and show even a higher intrinsic field enhancement than Au. However, the synthesis of stable monodisperse AgNPs is much more difficult to achieve.

In view of the steadily growing importance of SERR spectroscopy in biological application, the preservation of the native structure constitutes an additional requirement on the design of nanoparticles. Biocompatible coatings on nanoparticles that may protect proteins against direct and usually harmful interactions with the metal can be obtained by self-assembled monolayers (SAMs) of ω-functionalised mercaptoalkanes.[3]

Again, this method has been established for Au but, up to now, only one SERR spectroscopic study of proteins on SAM-coated AgNPs has been reported.[4] However, in that work rather unstable AgNP aggregates were used. In addition, the yield of SAM coating was very low and no information about the integrity of the immobilised protein could be provided.

In the present work, we have thus established a procedure to prepare small sized SAM-coated AgNPs, starting with citrate-capped seeds that were subsequently grown for controlled size adjustment[5] and post-functionalised for biocompatible protein attachment. Using cytochrome *c* (Cyt-*c*), a well-characterized model protein frequently used in SERR spectroscopy,[6] we have systematically investigated how selective sensitivity of the particles can be improved and structural integrity of immobilised proteins is ensured. The optical properties of the AgNPs were tuned such that their plasmonic resonance matches the Soret transition of the Cyt *c* heme cofactor at 410 nm.[7]

First, citrate-capped AgNPs were prepared by borohydride reduction of Ag^+ ions in the presence of citrate (Fig. S1, ESI‡). The UV-vis spectrum displays a sharp SPR peak at 390 nm, indicating that no aggregates are formed. The NPs were almost spherical with an aspect ratio, defined as the ratio between the longer and the shorter particle axis, of $R = 1.04 \pm 0.005$. For the longer axis a mean diameter of 12 ± 0.4 nm was determined (Fig. S2, ESI‡). These particles were subsequently used as seeds for preparing AgNPs of larger size *via* the seeding growth method:[8] $AgNO_3$ was added to the seed solution containing citrate-capped AgNPs and ascorbic acid (AA) as the reducing agent. The growth of the particle could be controlled by the concentrations of $AgNO_3$ and AA (Fig. S2 and S3, ESI‡). The AgNPs were functionalised by stirring a solution containing citrate-capped AgNPs and mercaptoundecanoic acid (MUA) at different concentrations over night. In the last step, Cyt *c* was added to a final concentration between 0.05–1.3 μM. SERR spectra of Cyt *c* were measured with the 413-nm excitation line of a Kr^+ laser using a confocal Raman spectrometer or a spectrograph operating in a 90° scattering geometry (for further experimental details, see ESI‡).

Technische Universität Berlin, Institut für Chemie, Sekr. PC 14, Straße des 17. Juni 135, D-10623 Berlin, Germany. E-mail: i.weidinger@mailbox.tu-berlin.de; Fax: +49 3031421122; Tel: +49 3031422780

† This article is part of a ChemComm web-based themed issue on Surface Enhanced Raman Spectroscopy.

‡ Electronic supplementary information (ESI) available: Experimental details and additional TEM and spectroscopic data for further AgNP characterisation. See DOI: 10.1039/c0cc05058j

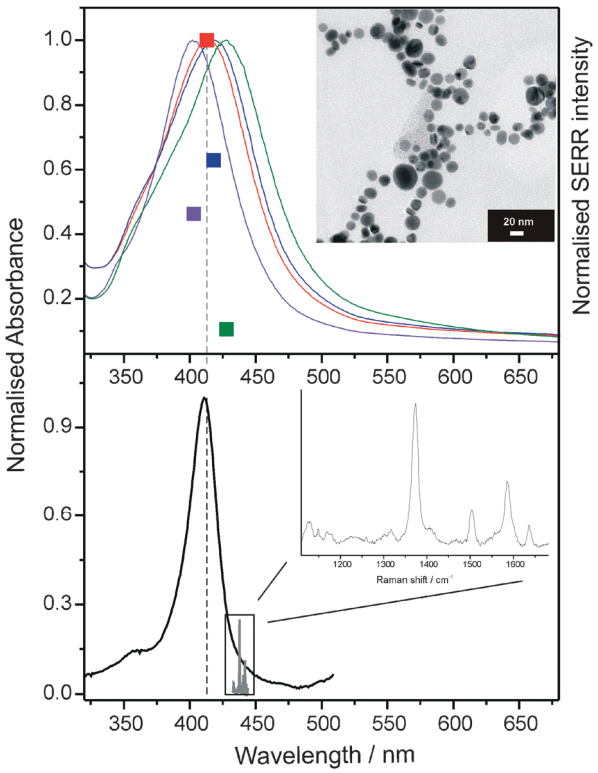

Fig. 1 Top: UV-Vis spectra of MUA–AgNPs with λ_{max} = 403 (violet), 413 (red), 418 (blue) and 427 (green) nm. SERR intensity (squares) of the maximum Raman band (ν_4) of adsorbed Cyt *c* as a function of λ_{max}. Inset: TEM picture of MUA–AgNP with SPR at 413 nm. Bottom: UV-vis spectrum of Cyt *c* at the Soret band region (solid line). Inset: SERR spectrum of Cyt *c*.

The SPR position of a given nanoparticle ensemble can be monitored by UV-visible absorption spectroscopy. Fig. 1 (top) shows the UV-vis spectra of 4 different nanoparticle batches obtained with different growth solutions. As a consequence of the particle seeding and coating, the SPR is different for each batch, *i.e.* at 403, 413, 418 and 427 nm. The red shift from 390 nm to 403 nm can solely be attributed to the MUA coating that increases the local dielectric constant of the surrounding medium. Correspondingly for all nanoparticle batches a shift of 13 nm was observed after MUA addition. Further SPR tuning to 413, 418 and 427 nm was achieved by adding $AgNO_3$ of different concentrations to the nanoparticle seed solution which led to an increase in average size and aspect ratio (Fig. S3, ESI‡). Both effects are generally assumed to cause a red shift of the SPR position.[1,2,9]

Addition of Cyt *c* to the AgNP solution leads to a further red shift of the SPR by 8–10 nm (Fig. S3, ESI‡), indicating that the protein was effectively adsorbed on the NP surface. In all cases, a time-dependent drop in plasmon absorption intensity was observed which is attributed to a slow aggregation of the nanoparticles upon Cyt *c* binding. Surprisingly the Ag_{413}/Cyt *c* complex was stable even after 90 min whereas the Ag_{427} nanoparticle batch completely lost plasmonic activity already 15 min after Cyt *c* addition.

Fig. 1 (top squares) also shows the normalised SERR intensity of Cyt *c* adsorbed on the various MUA-coated AgNPs. The highest intensity is obtained for the Ag_{413}NPs where the SPR maximum coincidences with the excitation energy. The SERR intensity strongly decreases for NPs with SPR maxima at lower and higher wavelengths. In the latter case, namely for Ag_{418} and Ag_{427}, the weaker signal enhancement may be mainly due to the strong tendency of the particles to aggregate upon Cyt *c* addition. Nevertheless, the results clearly show that a good SERR intensity can only be achieved in a small spectral window where the SPR matches the molecular electronic transition of the heme cofactor of the protein.

Citrate-reduced AgNPs have been shown to afford high SERR signal intensities of the adsorbed Cyt *c*.[10] However, the high charge density of the citrate layer causes irreversible denaturation of the protein which, in the case of Cyt *c*, is reflected by the transition from the native six-coordinated low spin (6cLS) configuration to a five-coordinated high spin (5cHS) species in the SERR spectrum.[6] Replacing citrate by MUA is expected to improve the stability of the native protein structure. This is in fact confirmed by the present results although the preservation of the protein structure depends on the conditions of SAM formation, specifically on the MUA concentration used for citrate/MUA exchange (Fig. 2). Using a molar MUA/AgNP ratio of *ca.* 10^4, the citrate/MUA exchange is not complete as concluded from the residual contribution of the 5cHS species in the SERR spectrum which is reflected by the characteristic marker band at 1490 cm^{-1} (ν_3). Upon increasing the MUA/AgNP ratio to 10^6, the SERR spectrum of the bound Cyt *c* exhibits essentially the same vibrational signature as the resonance Raman (RR) spectrum of Cyt *c* in solution. The preservation of the proteins native structure, however, is achieved at the expense of the SERR

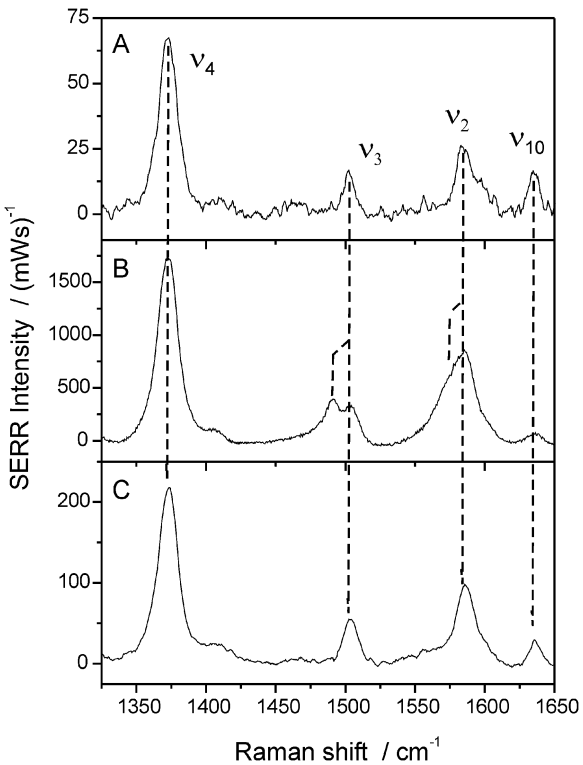

Fig. 2 (A) RR spectrum of Cyt *c* in solution (20 μM) compared with the SERR spectra of Cyt *c* bound to SAM-coated AgNPs (1 μM Cyt *c*) using MUA/AgNP ratios of *ca.* 10^4 (B) and 10^6 (C).

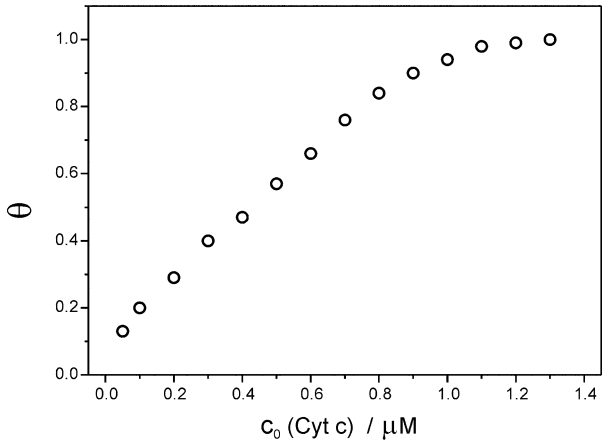

Fig. 3 Relative Cyt *c* surface coverage as a function of protein concentration in solution.

intensity which is *ca.* one order of magnitude lower than for the citrate-capped AgNPs due to the larger separation of the protein from the Ag surface.

The surface coverage of Cyt *c* was determined by monitoring SERR intensity of Cyt *c* for different protein concentrations in solution. The relative surface concentration is given by: $\theta = \Gamma/\Gamma_S$, where Γ and Γ_S refer to the surface coverage at a particular Cyt *c* concentration and to the saturation surface coverage, respectively. θ was calculated by $\theta = I_{SERRS}/I^{max}_{SERRS}$ and plotted as a function of initial Cyt *c* concentration c_0 in solution (Fig. 3) . At low c_0 (<1 μM), θ increases linearly with c_0 but it levels off for $c_0 > 1$ μM. The data could be well described by a fit of a Langmuir adsorption isotherm:

$$\theta = \frac{K \cdot c}{1 + K \cdot c} \qquad (1)$$

where K is the equilibrium constant and $c = c_0 - \theta\Gamma_s$ corresponds to the Cyt concentration in solution after adsorption equilibrium is established. The fit of eqn (1) to the data in Fig. 3 affords $\Gamma_s = 0.86$ μM and $K = 1.2 \times 10^8$ M^{-1} (Fig. S4, ESI‡). Additional UV-vis spectroscopic determination of the solution concentration of Cyt *c* carried out with the supernatants of centrifuged MUA capped AgNP suspensions (Fig. S5, ESI‡) yields essentially the same result for Γ_s. Approximating an ideal spherical shape for the AgNPs and a diameter of *ca.* 17 nm we can estimate the NP concentration to be *ca.* 11 nM, leading to a surface coverage of roughly 80 Cyt *c* molecules per nanoparticle in the saturation limit. If we consider that the particle diameter is increased by *ca.* 4 nm due to the MUA coating the surface concentration of Cyt *c* is estimated to be 10 pM cm^{-2} which is in good agreement with the data obtained in a previous work on MUA-coated Au electrodes.[11] On the basis of these data, the Raman enhancement factor (REF) is determined according to

$$\mathrm{REF} = \frac{I_{SERRS} \cdot c_{RR}}{I_{RR} \cdot c_{SERRS} \cdot k} \qquad (2)$$

where c_{RR} is the Cyt *c* concentration used in the RR experiment, c_{SERR} refers to the concentration of the adsorbed Cyt *c* in the SERR experiments, determined according to eqn (1), and k is a shielding factor that is assumed to be 0.25 as discussed previously.[10] For determining the SERR and RR intensities of the 1373 cm^{-1} band (I_{SERR}, I_{RR}), the measurements were carried out with the AgNP/Cyt *c* suspensions and the Cyt *c* solution adjusted to the same optical density at the excitation wavelength. Thus, REF was determined to be $(1.3 \pm 0.4)10^2$. Taking into account that the MUA coating causes an attenuation of the surface enhancement by *ca.* one order of magnitude, the enhancement factor for the protein directly attached to the metal would be *ca.* 10^3. This factor is the product of the enhancement of the intensity of the incident and Raman scattered radiation at λ_{exc} and λ_{Raman}, respectively. For the Ag_{413}NPs considered here, the surface plasmon absorption exhibits its maximum at λ_{exc} but it has dropped to *ca.* 0.86 of this value at λ_{Raman}. Assuming that the enhancement intensity scales with the surface plasmon absorption, the enhancement factor for the incident electric field at λ_{exc} is estimated to be 37. This value is in very good agreement with the theoretically predicted enhancement of *ca.* 40 according to Zeman and Schatz.[9]

In conclusion, we have shown that by precise tuning of the plasmonic properties of AgNPs, SERR detection of specific cofactors in proteins is possible down to nanomolar concentrations. Coating of AgNPs by SAMs with appropriate head groups allows for binding of proteins under preservation of the native structure.

The authors would like to thank Peter Hildebrandt for helpful discussions and Soeren Selve from the ZELMI TU Berlin for the TEM pictures. Financial support from the Fonds der Chemie (IW), the Alfried Krupp Wissenschaftskolleg, Greifswald (AS) and the DFG (Unicat) is gratefully acknowledged.

Notes and references

1 S. Link and M. A. El-Sayed, *J. Phys. Chem. B*, 1999, **103**, 8410–8426.
2 K. L. Kelly, E. Coronado, L. L. Zhao and G. C. Schatz, *J. Phys. Chem. B*, 2003, **107**, 668–677.
3 G. H. Woehrle, L. O. Brown and J. E. Hutchison, *J. Am. Chem. Soc.*, 2005, **127**, 2172–2183.
4 A. Bonifacio, L. V. D. Sneppen, C. Gooijer and G. V. D. Zwan, *Langmuir*, 2004, **20**, 5858–5864.
5 K. R. Brown and M. J. Natan, *Langmuir*, 1998, **14**, 726–728.
6 S. Oellerich, H. Wackerbarth and P. Hildebrandt, *J. Phys. Chem. B*, 2002, **106**, 6566–6580.
7 D. H. Murgida and P. Hildebrandt, *Acc. Chem. Res.*, 2004, **37**, 854–861.
8 N. R. Jana, L. Gearheart and C. J. Murphy, *Langmuir*, 2001, **17**, 6782–6786.
9 E. J. Zeman and G. C. Schatz, *J. Phys. Chem.*, 1987, **91**, 634–643.
10 P. Hildebrandt and M. Stockburger, *J. Phys. Chem.*, 1986, **90**, 6017–6024.
11 S. Song, R. A. Clark, E. F. Bowden and M. J. Tarlov, *J. Phys. Chem.*, 1993, **97**, 6564–6572.